

Supporting Information

Triplet Energy vs Electron Transfers in Porphyrin- and Tetrabenzoporphyrin-carboxylates/Pd₃(dppm)₃(CO)²⁺ Cluster Assemblies; A Question of Negative Charge

Peng Luo,^a Paul-Ludovic Karsenti,^a Benoit Marsan^{b*} and Pierre D. Harvey^{a*}

^aDépartement de chimie, Université de Sherbrooke, Sherbrooke, QC, J1K 2R1, Canada.

^bDépartement de chimie, Université du Québec à Montréal, Montréal, QC, H2X 2J6, Canada.

Table of Content

Table S1. Phosphorescence lifetimes for TCPP and TCPBP in 1:1 MeOH:2MeTHF mixture with increasing amount of $[Pd_3^{2+}]$ at 77 K.	S2
Figure S1. Top left: variation of phosphorescence spectra of TCPP (1.02×10^{-5} M) upon adding $[Pd_3^{2+}]$ in 1:1 MeOH:2MeTHF at 77 K. Curves A-J were obtained with successive addition of $[Pd_3^{2+}]$. Each curve represents an increase in $[Pd_3^{2+}]$ concentration by 3.65×10^{-6} for TCPP . Top right: relative decrease of intensity with respect to the starting intensity. Middle left: plot of (Φ_p°/Φ_p) vs $[Pd_3^{2+}]$ (<i>i.e.</i> Stern-Volmer plot). Middle right: graph of $\log[(\Phi_p^\circ - \Phi_p)/\Phi_p]$ vs $\log[Pd_3^{2+}]$. Bottom left: graph of $[1 - (\Phi_p/\Phi_p^\circ)]/[Pd_3^{2+}]$ vs (Φ_p/Φ_p°) . Bottom right: graph of $\ln(W)$ vs $[Pd_3^{2+}]$ for TCPP ••• $[Pd_3^{2+}]_x$ assembly in 1:1 MeOH:2MeTHF at 77 K.	S3
Figure S2. Top left: variation of phosphorescence spectra of TCPEP (5.50×10^{-6} M) upon adding $[Pd_3^{2+}]$ in 1:1 MeOH:2MeTHF at 77 K. Curves A-J were obtained with successive addition of $[Pd_3^{2+}]$. Each curve represents an increase in $[Pd_3^{2+}]$ concentration by 2.11×10^{-6} for TCPEP . Top right: relative decrease of intensity with respect to the starting intensity. Middle left: plot of (Φ_p°/Φ_p) vs $[Pd_3^{2+}]$ (<i>i.e.</i> Stern-Volmer plot). Middle right: graph of $\log[(\Phi_p^\circ - \Phi_p)/\Phi_p]$ vs $\log[Pd_3^{2+}]$. Bottom left: graph of $[1 - (\Phi_p/\Phi_p^\circ)]/[Pd_3^{2+}]$ vs (Φ_p/Φ_p°) . Bottom right: graph of $\ln(W)$ vs $[Pd_3^{2+}]$ for TCPEP ••• $[Pd_3^{2+}]_x$ assembly in 1:1 MeOH:2MeTHF at 77 K.	S4
Figure S3. Top left: variation of phosphorescence spectra of TCPEBP (7.78×10^{-6} M) upon adding $[Pd_3^{2+}]$ in 1:1 MeOH:2MeTHF at 77 K. Note that the phosphorescence peaks do not move upon changing the excitation wavelength. Curves A-J were obtained with successive addition of $[Pd_3^{2+}]$. Each curve represents an increase in $[Pd_3^{2+}]$ concentration by 5.67×10^{-5} for TCPEBP . Top right: relative decrease of intensity with respect to the starting intensity. Middle left: plot of (Φ_p°/Φ_p) vs $[Pd_3^{2+}]$ (<i>i.e.</i> Stern-Volmer plot). Middle right: graph of $\log[(\Phi_p^\circ - \Phi_p)/\Phi_p]$ vs $\log[Pd_3^{2+}]$. Bottom left: graph of $[1 - (\Phi_p/\Phi_p^\circ)]/[Pd_3^{2+}]$ vs (Φ_p/Φ_p°) . Bottom right: graph of $\ln(W)$ vs $[Pd_3^{2+}]$ for TCPEBP ••• $[Pd_3^{2+}]_x$ assembly in 1:1 MeOH:2MeTHF at 77 K.	S5
Figure S4. Optimized triplet geometry of TCPP (as Na ⁺ salt) in a MeOH solvent field.	S6
Figure S5. Representations of the semi-occupied frontier MOs of TCPP (Na ⁺ salt).	S6
Table S2. Evaluation of the (S ₀ -T ₁) energy gap for TCPP .	S6
Figure S6. Optimized triplet geometry of TCPBP (Na ⁺ salt) in MeOH solvent field.	S6
Figure S7. Representations of the semi-occupied frontier MOs of TCPBP (Na ⁺ salt).	S7
Table S3. Evaluation of the (S ₀ -T ₁) energy gap for TCPBP .	S7
Figure S8. Optimized triplet geometry of TCPEP (Na ⁺ salt) in MeOH solvent field.	S7

Figure S9. Representations of the semi-occupied frontier MOs of TCPEP (as Na^+ salt).	S7
Table S4. Evaluation of the (S_0 - T_1) energy gap for TCPEP in a MeOH solvent field.	S8
Figure S10. Optimized triplet geometry of TCPEBP (as Na^+ salt) in a MeOH solvent field.	S8
Figure S11. Representations of the semi-occupied frontier MOs of TCPEBP (as Na^+ salt).	S8
Table S5. Evaluation of the (S_0 - T_1) energy gap for TCPEBP .	S8
Figure S12. Optimized triplet geometry of the TCPP •••[Pd_3^{2+}] assembly in a MeOH solvent field.	S8
Figure S13. Representations of the semi-occupied frontier MOs of the TCPP •••[Pd_3^{2+}] assembly.	S9
Table S6. Comparison of selected calculated distances in the TCPP •••[Pd_3^{2+}] assembly.	S9
Figure S14. Representations of the semi-occupied frontier MOs of the TCPBP •••[Pd_3^{2+}] assembly.	S9
Table S7. Comparison of selected calculated distances in the TCPBP •••[Pd_3^{2+}] assembly.	S10
Figure S15. Optimized triplet geometry of the TCPEP •••[Pd_3^{2+}] assembly in MeOH solvent field.	S10
Figure S16. Representations of the semi-occupied frontier MOs of the TCPEP •••[Pd_3^{2+}] assembly.	S10
Table S8. Comparison of selected calculated distances in the TCPEP •••[Pd_3^{2+}] assembly.	S10
Table S9. Comparison of selected calculated distances in the TCPEBP •••[Pd_3^{2+}] assembly.	S11
Figure S17. Monitoring of the transient signals of TCPP , TCPEP and PCPEBP in 2MeTHF in the presence of 2 equiv. of [Pd_3^{2+}] at 298 K.	S11

Table S1. Phosphorescence lifetimes for **TCPP** and **TCPBP** in 1:1 MeOH:2MeTHF mixture with increasing amount of [Pd_3^{2+}] at 77 K.

Porphyrins vs [Pd_3^{2+}]	TCPP (ms)	TCPBP (ms)
1:0	25.18±0.47	24.20±0.44
1:0.25	25.14±0.42	24.17±0.49
1:0.5	25.10±0.37	24.12±0.48
1:0.75	25.06±0.38	24.07±0.55
1:1	25.01±0.44	24.03±0.50

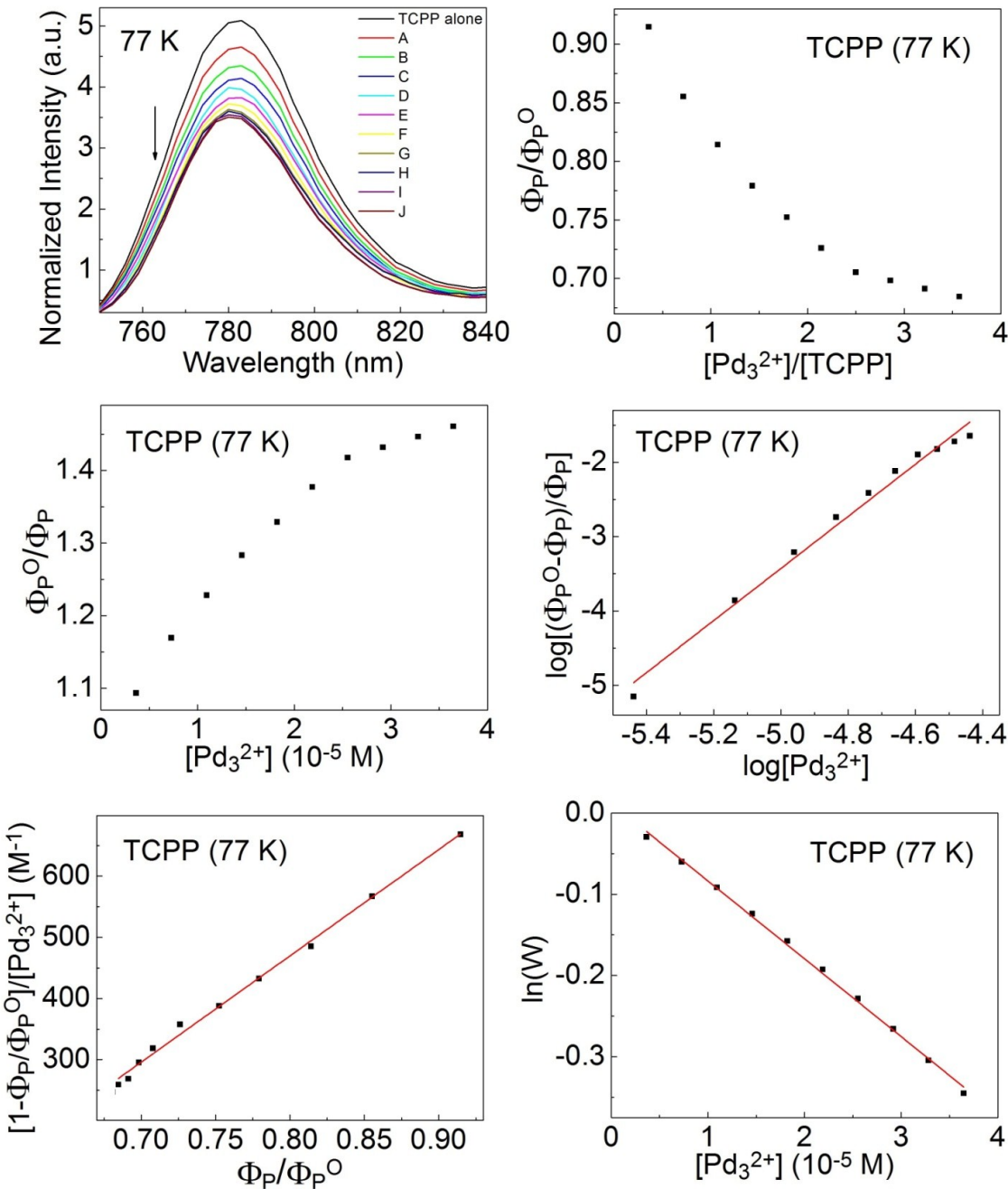


Figure S1. Top left: variation of phosphorescence spectra of **TCPP** ($1.02 \times 10^{-5} M$) upon adding $[Pd_3^{2+}]$ in 1:1 MeOH:2MeTHF at 77 K. Curves A-J were obtained with successive addition of $[Pd_3^{2+}]$. Each curve represents an increase in $[Pd_3^{2+}]$ concentration by 3.65×10^{-6} for **TCPP**. Top right: relative decrease of intensity with respect to the starting intensity. Middle left: plot of (Φ_{P^0}/Φ_P) vs $[Pd_3^{2+}]$ (*i.e.* Stern-Volmer plot). Middle right: graph of $\log[(\Phi_{P^0}-\Phi_P)/\Phi_P]$ vs $\log[Pd_3^{2+}]$. Bottom left: graph of $[1-(\Phi_P/\Phi_{P^0})]/[Pd_3^{2+}]$ vs (Φ_P/Φ_{P^0}) . Bottom right: graph of $\ln(W)$ vs $[Pd_3^{2+}]$ for $\text{TCPP}\cdots[Pd_3^{2+}]_x$ assembly in 1:1 MeOH:2MeTHF at 77 K.

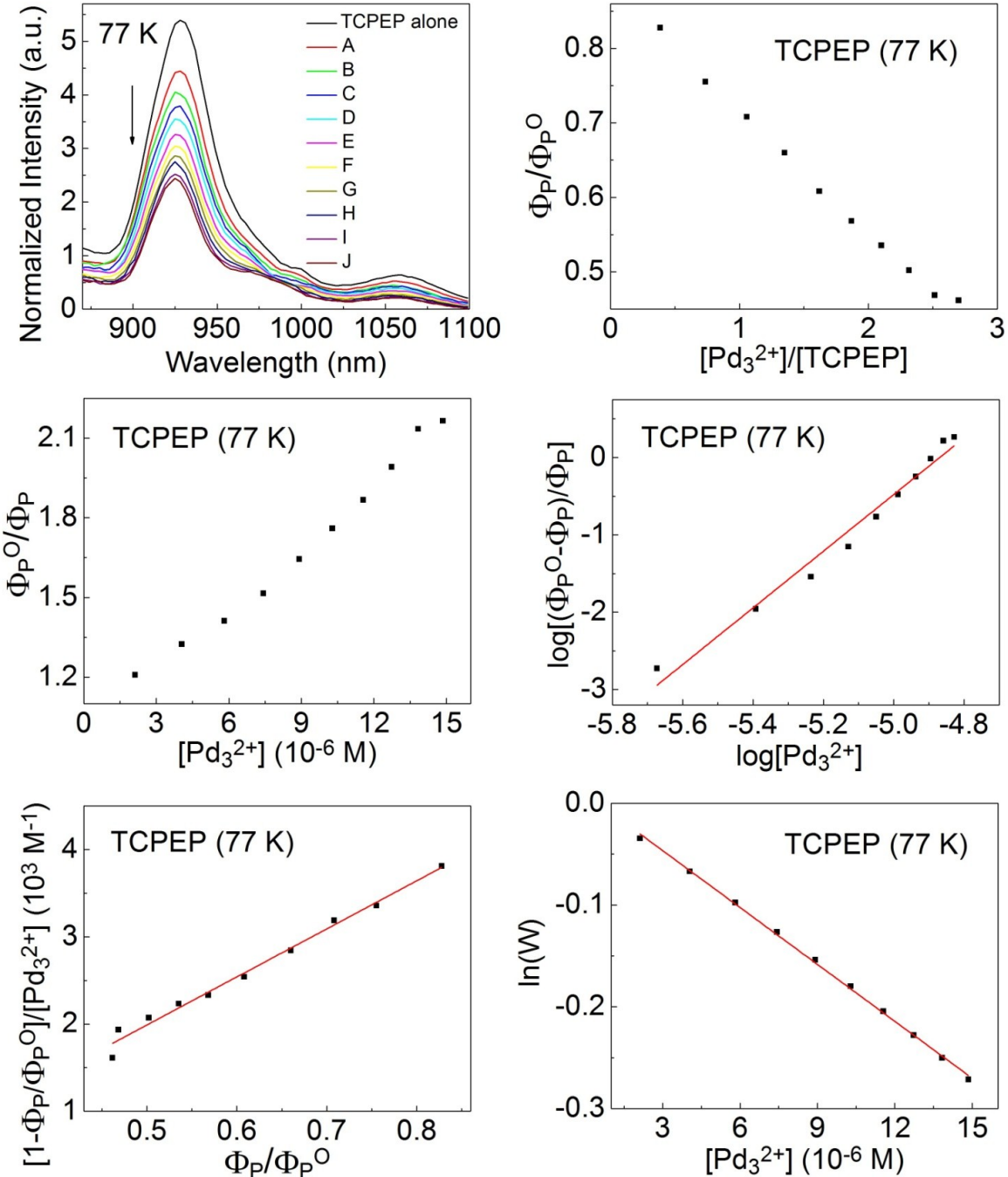


Figure S2. Top left: variation of phosphorescence spectra of TCPEP (5.50×10^{-6} M) upon adding $[Pd_3^{2+}]$ in 1:1 MeOH:2MeTHF at 77 K. Curves A-J were obtained with successive addition of $[Pd_3^{2+}]$. Each curve represents an increase in $[Pd_3^{2+}]$ concentration by 2.11×10^{-6} M for TCPEP. Top right: relative decrease of intensity with respect to the starting intensity. Middle left: plot of (Φ_P^0/Φ_P) vs $[Pd_3^{2+}]$ (i.e. Stern-Volmer plot). Middle right: graph of $\log[(\Phi_P^0 - \Phi_P)/\Phi_P]$ vs $\log[Pd_3^{2+}]$. Bottom left: graph of $[1 - (\Phi_P/\Phi_P^0)] / [Pd_3^{2+}]$ vs (Φ_P/Φ_P^0) . Bottom right: graph of $\ln(W)$ vs $[Pd_3^{2+}]$ for $TCPEP \cdots [Pd_3^{2+}]_x$ assembly in 1:1 MeOH:2MeTHF at 77 K.

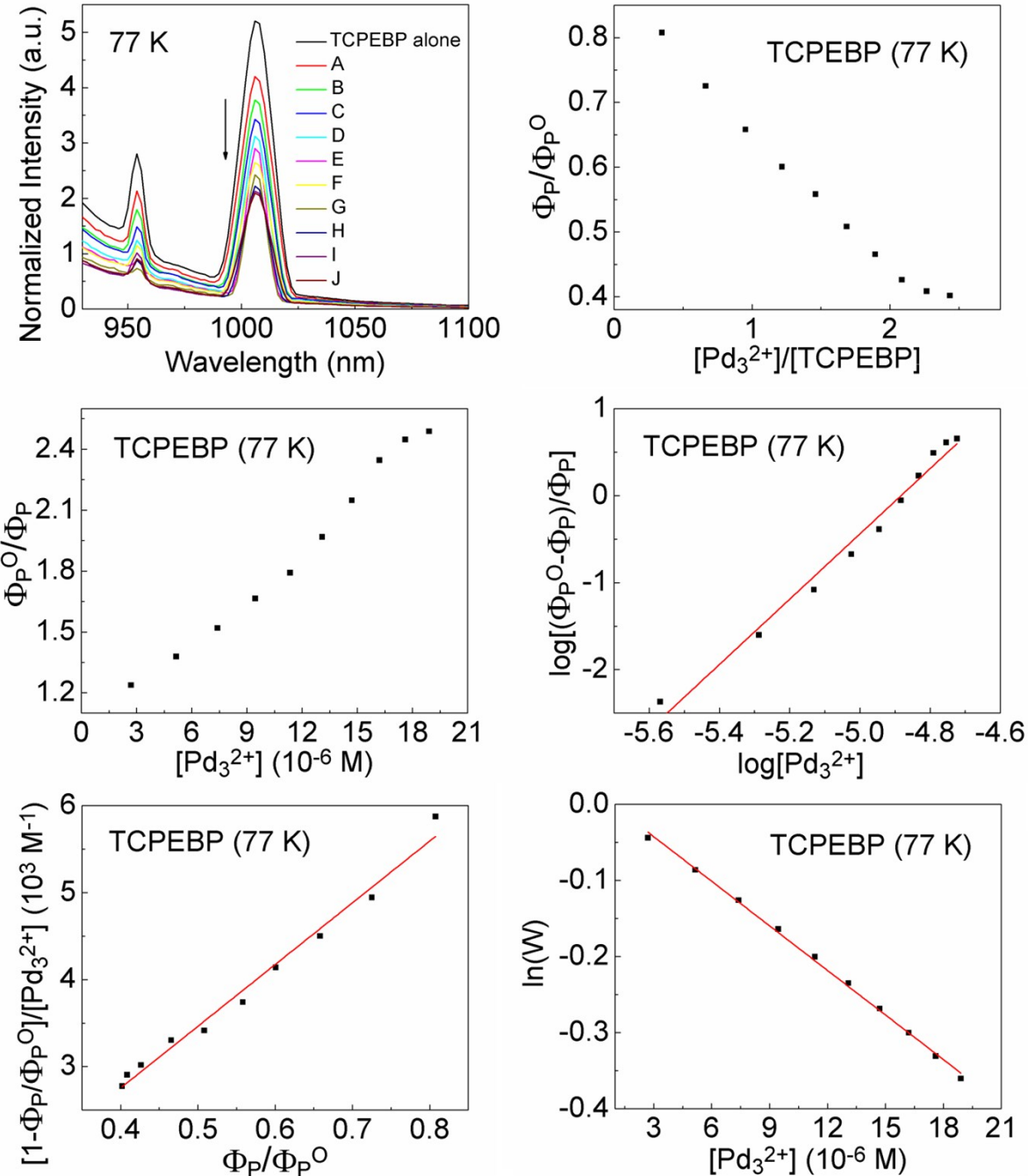


Figure S3. Top left: variation of phosphorescence spectra of **TCPEBP** (7.78×10^{-6} M) upon adding $[Pd_3^{2+}]$ in 1:1 MeOH:2MeTHF at 77 K. Note that the phosphorescence peaks do not move upon changing the excitation wavelength. Curves A-J were obtained with successive addition of $[Pd_3^{2+}]$. Each curve represents an increase in $[Pd_3^{2+}]$ concentration by 5.67×10^{-5} M for **TCPEBP**. Top right: relative decrease of intensity with respect to the starting intensity. Middle left: plot of (Φ_P^0/Φ_P) vs $[Pd_3^{2+}]$ (i.e. Stern-Volmer plot). Middle right: graph of $\log[(\Phi_P^0 - \Phi_P)/\Phi_P]$ vs $\log[Pd_3^{2+}]$. Bottom left: graph of $[1 - (\Phi_P/\Phi_P^0)]/[Pd_3^{2+}]$ vs (Φ_P/Φ_P^0) . Bottom right: graph of $\ln(W)$ vs $[Pd_3^{2+}]$ for **TCPEBP**••• $[Pd_3^{2+}]_x$ assembly in 1:1 MeOH:2MeTHF at 77 K.

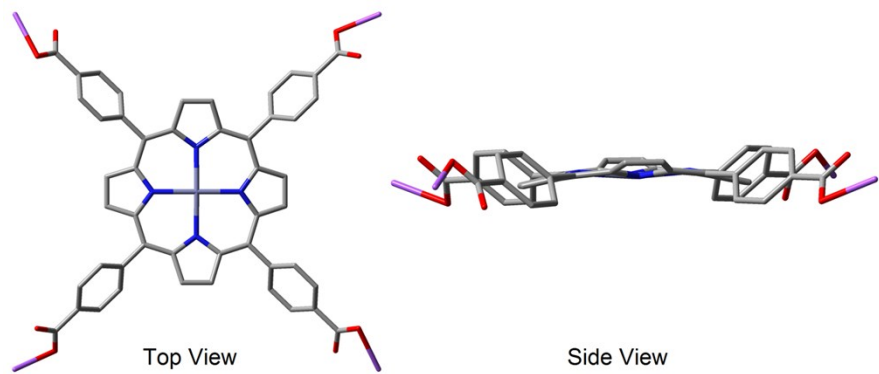


Figure S4. Optimized triplet geometry of **TCPP** (as Na^+ salt) in a MeOH solvent field.

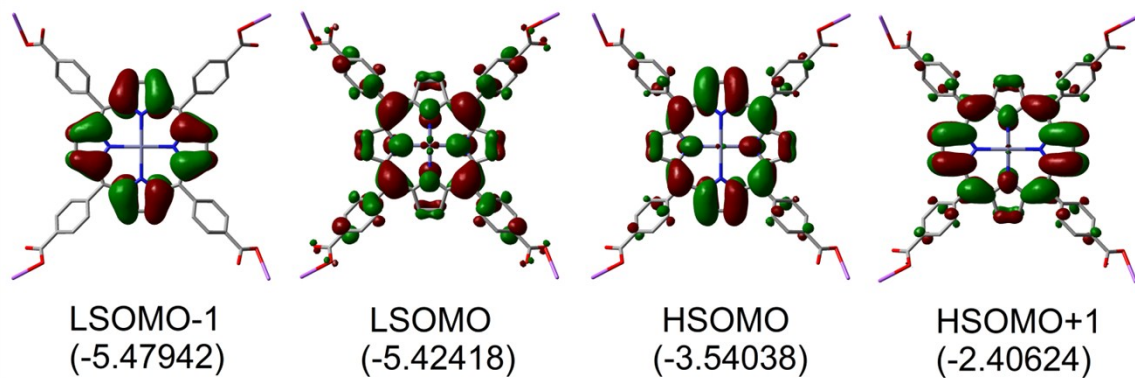


Figure S5. Representations of the semi-occupied frontier MOs of **TCPP** (Na^+ salt) in MeOH solvent field (energies in eV).

Table S2. Evaluation of the (S_0 - T_1) energy gap for **TCPP**.

	Singlet S_0 (a.u.)	Triplet T_1 (a.u.)	(S_0-T_1) (a.u.)	(S_0-T_1) (eV)	Computed position of phosphorescence (nm)
TCPP	-3540.21912	-3540.16192	0.05720	1.55653	797

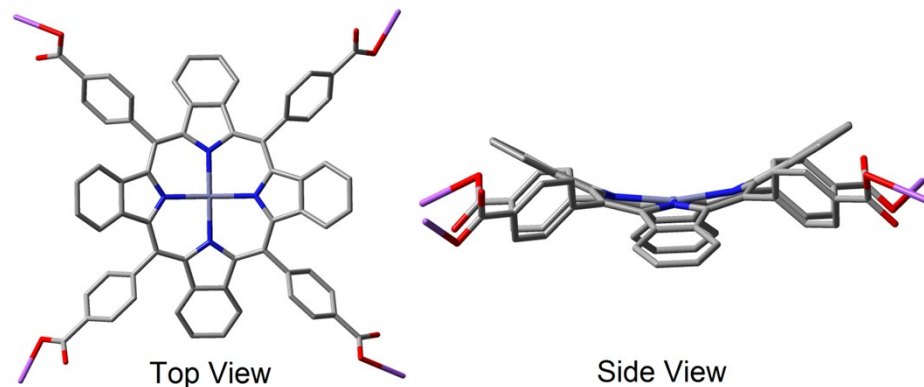


Figure S6. Optimized triplet geometry of **TCPBP** (Na^+ salt) in MeOH solvent field.

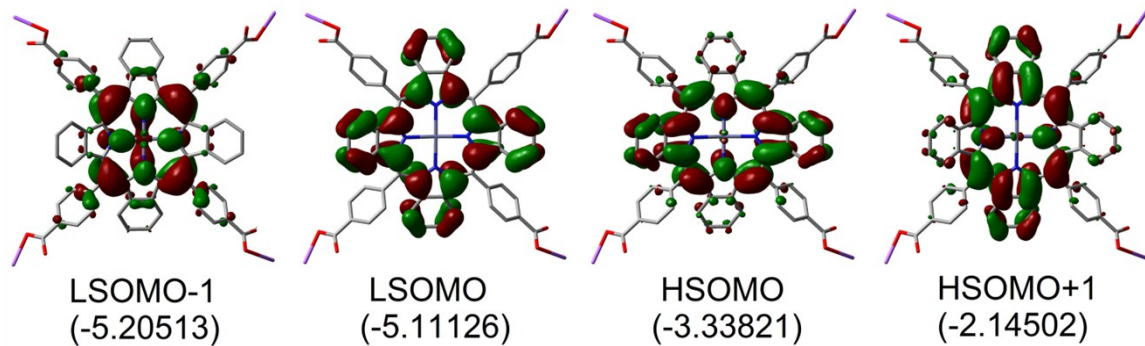


Figure S7. Representations of the semi-occupied frontier MOs of **TCPBP** (Na^+ salt) in MeOH solvent field (energies in eV).

Table S3. Evaluation of the (S_0 - T_1) energy gap for **TCPBP**.

	Singlet S_0 (a.u.)	Triplet T_1 (a.u.)	(S_0-T_1) (a.u.)	(S_0-T_1) (eV)	Computed position of phosphorescence (nm)
TCPBP	-4154.76960	-4154.71623	0.05337	1.45227	855

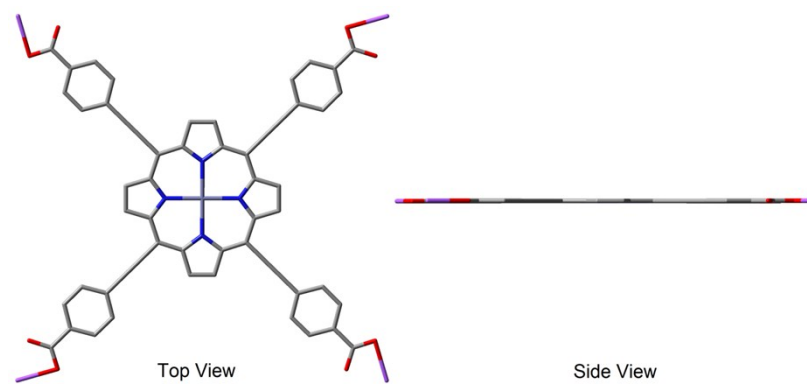


Figure S8. Optimized triplet geometry of **TCPEP** (Na^+ salt) in MeOH solvent field.

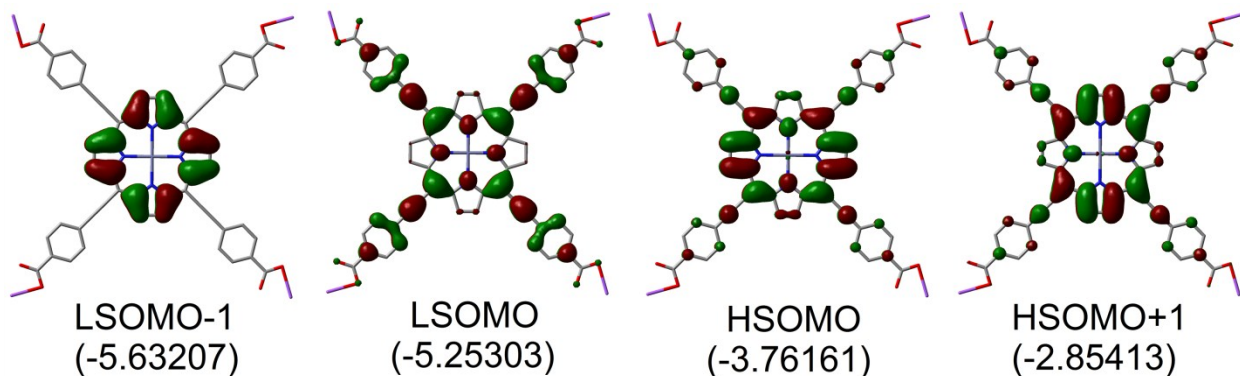


Figure S9. Representations of the semi-occupied frontier MOs of **TCPEP** (as Na^+ salt) in a MeOH solvent field (energies in eV).

Table S4. Evaluation of the (S_0-T_1) energy gap for **TCPEP** in a MeOH solvent field.

	Singlet S_0 (a.u.)	Triplet T_1 (a.u.)	(S_0-T_1) (a.u.)	(S_0-T_1) (eV)	Computed position of phosphorescence (nm)
TCPEP	-3844.86559	-3844.81791	0.04768	1.29750	957

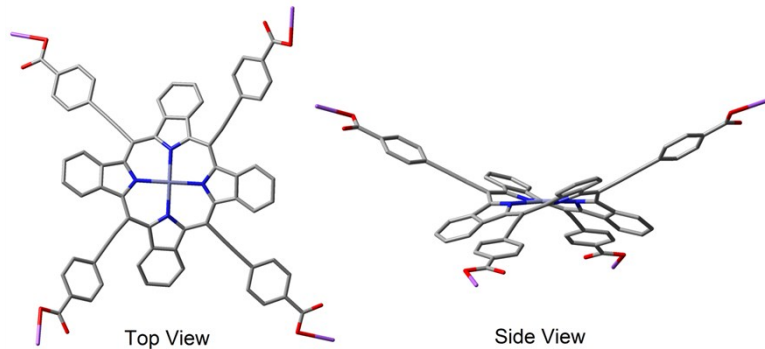


Figure S10. Optimized triplet geometry of **TCPEBP** (as Na^+ salt) in a MeOH solvent field.

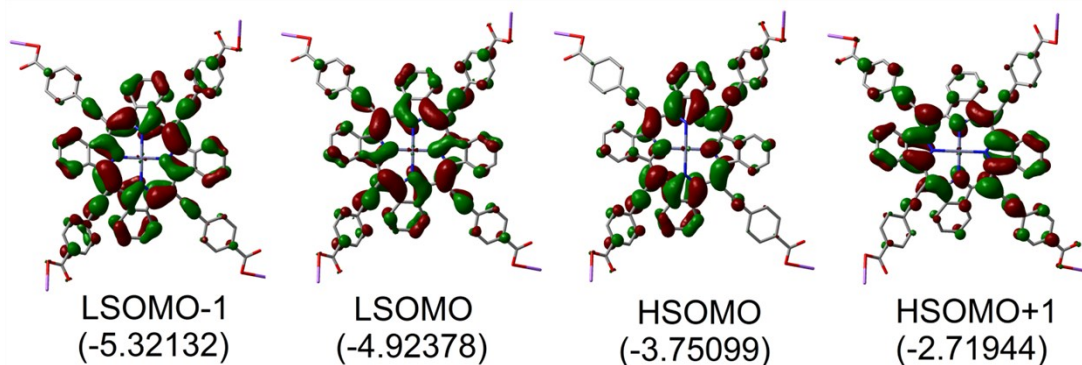


Figure S11. Representations of the semi-occupied frontier MOs of **TCPEBP** (as Na^+ salt) in a MeOH solvent field (energies in eV).

Table S5. Evaluation of the (S_0-T_1) energy gap for **TCPEBP**.

	Singlet S_0 (a.u.)	Triplet T_1 (a.u.)	(S_0-T_1) (a.u.)	(S_0-T_1) (eV)	Computed position of phosphorescence (nm)
TCPEBP	-4459.41685	-4459.37301	0.04384	1.19282	1041

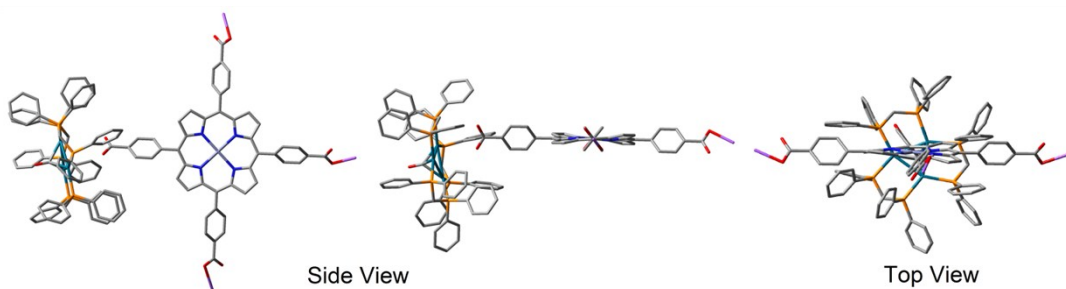


Figure S12. Optimized triplet geometry of the $\text{TCPP}\bullet\bullet[\text{Pd}_3^{2+}]$ assembly in a MeOH solvent field.

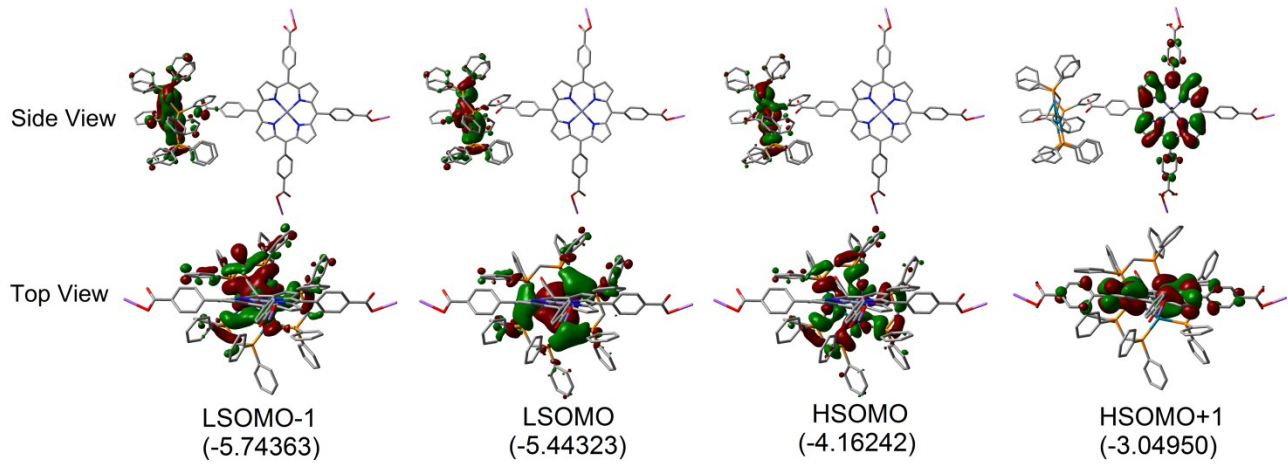


Figure S13. Representations of the semi-occupied frontier MOs of the **TCPP**...[Pd_3^{2+}] assembly in MeOH solvent field (energies in eV).

Table S6. Comparison of selected calculated distances in the **TCPP**...[Pd_3^{2+}] assembly.

	Singlet S_0 (\AA) ^a	Triplet T_1 (\AA)
Pd-Pd	2.706, 2.696, 2.690 (av.=2.697)	2.829, 2.819, 2.802 (av.=2.817)
Pd-P	2.415, 2.408, 2.405, 2.401, 2.398, 2.394 (av.=2.404)	2.446, 2.430, 2.428, 2.426, 2.425, 2.422 (av.=2.430)
Pd...O	1 st O: 3.861, 3.754, 3.608 (av.=3.741) 2 nd O: 5.605, 4.447, 4.444 (av.=4.832)	1 st O: 4.002, 3.711, 3.031 (av.=3.581) 2 nd O: 5.842, 4.747, 3.711 (av.=4.767)
Pd...Zn	13.580, 13.339, 13.326 (av.=13.415)	13.472, 13.361, 13.165 (av.=13.333)

^aFrom reference 22b of the text.

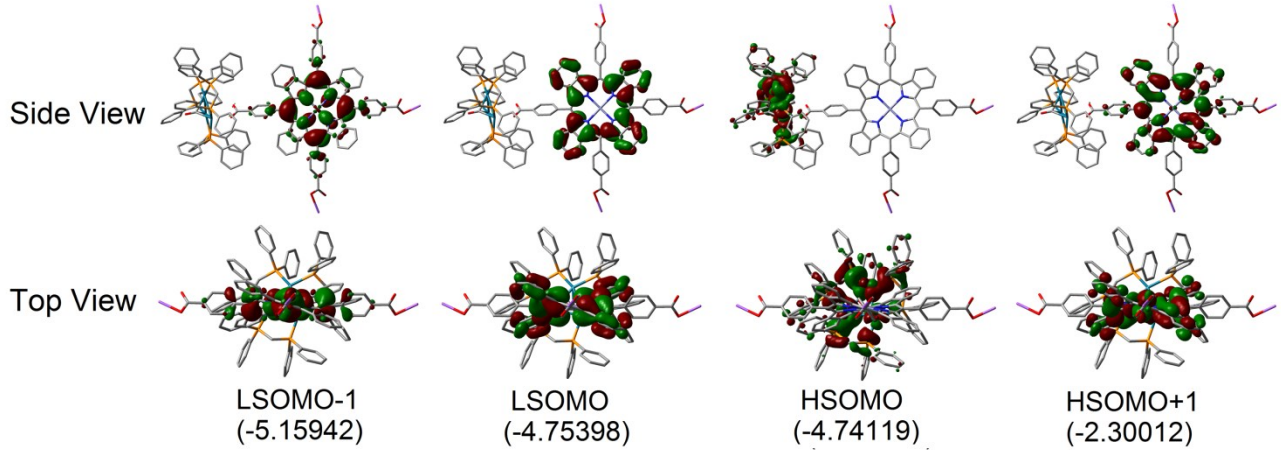
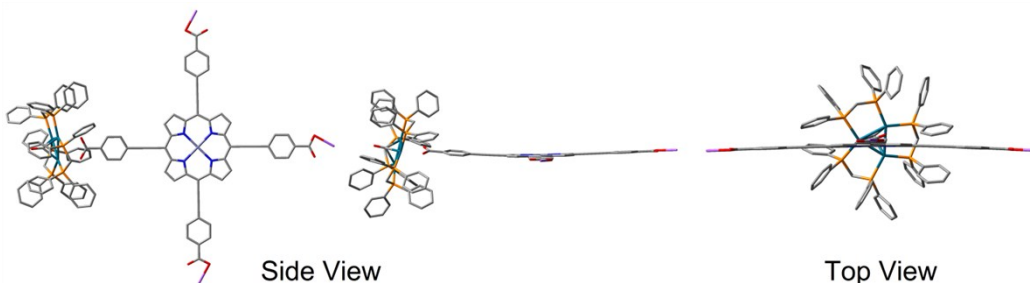
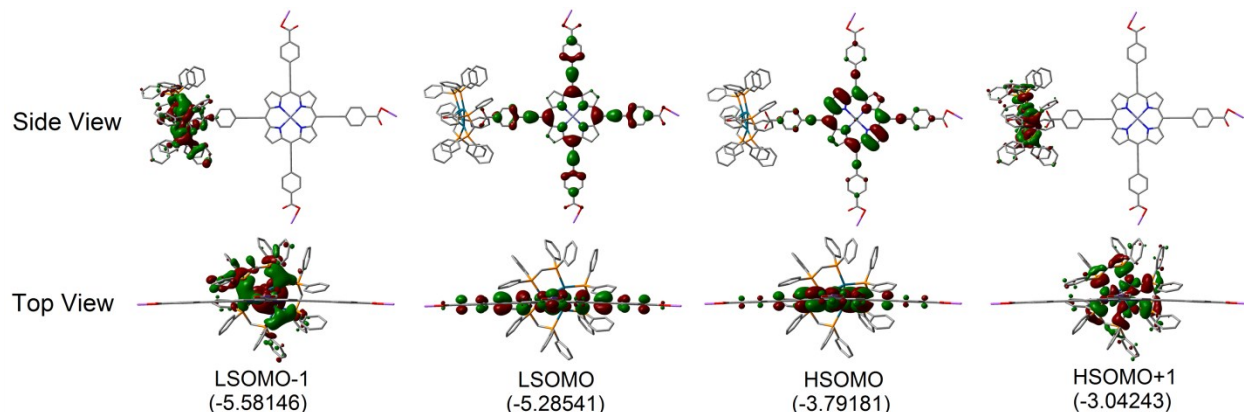


Figure S14. Representations of the semi-occupied frontier MOs of the **TCPBP**...[Pd_3^{2+}] assembly in MeOH solvent field (energies in eV).

Table S7. Comparison of selected calculated distances in the **TCPB^P•••[Pd₃²⁺]** assembly.

	Singlet S ₀ (Å) ^a	Triplet T ₁ (Å)
Pd-Pd	2.702, 2.691, 2.675 (av.=2.689)	2.934, 2.885, 2.795 (av.=2.871)
Pd-P	2.449, 2.438, 2.403, 2.397, 2.392, 2.389 (av.=2.411)	2.501, 2.469, 2.459, 2.456, 2.413, 2.399 (av.=2.450)
Pd•••O	1 st O: 3.645, 3.631, 3.485 (av.=3.587) 2 nd O: 4.055, 3.745, 3.443 (av.=3.748)	1 st O: 3.648, 3.545, 3.204 (av.=3.466) 2 nd O: 4.209, 3.401, 3.303 (av.=3.638)
Pd•••Zn	13.340, 13.025, 12.354 (av.=12.906)	13.195, 13.083, 12.209 (av.=12.829)

^aFrom reference 22b.of the text.

**Figure S15.** Optimized triplet geometry of the **TCPEP•••[Pd₃²⁺]** assembly in MeOH solvent field.**Figure S16.** Representations of the semi-occupied frontier MOs of the **TCPEP•••[Pd₃²⁺]** assembly in MeOH solvent field (energies in eV).**Table S8.** Comparison of selected calculated distances in the **TCPEP•••[Pd₃²⁺]** assembly.

	Singlet S ₀ (Å) ^a	Triplet T ₁ (Å)
Pd-Pd	2.682, 2.675, 2.670 (av.=2.676)	2.829, 2.819, 2.802 (av.=2.817)
Pd-P	2.443, 2.413, 2.409, 2.408, 2.399, 2.380 (av.=2.409)	2.446, 2.430, 2.428, 2.426, 2.425, 2.422 (av.=2.430)
Pd•••O	1 st O: 3.617, 3.438, 3.079 (av.=3.378) 2 nd O: 3.868, 3.573, 3.056 (av.=3.499)	1 st O: 3.602, 3.211, 3.031 (av.=3.281) 2 nd O: 3.642, 3.447, 3.011 (av.=3.367)
Pd•••Zn	15,582, 14.998, 14.956 (av.=15.179)	15,478, 14.893, 14.855 (av.=15.075)

^aFrom reference 22c of the text.

Table S9. Comparison of selected calculated distances in the **TCPEBP** \cdots [Pd₃²⁺] assembly.

	Singlet S ₀ (Å) ^a	Triplet T ₁ (Å)
Pd-Pd	2.707, 2.695, 2.678 (av.=2.693)	2.841, 2.807, 2.804 (av.=2.817)
Pd-P	2.433, 2.411, 2.407, 2.396, 2.395, 2.392 (av.=2.406)	2.453, 2.439, 2.431, 2.431, 2.429, 2.417 (av.=2.433)
Pd \cdots O	1 st O: 3.543, 3.213, 2.896 (av.=3.217) 2 nd O: 3.696, 3.184, 3.023 (av.=3.301)	1 st O: 3.296, 3.153, 3.041 (av.=3.163) 2 nd O: 3.530, 3.372, 2.803 (av.=3.235)
Pd \cdots Zn	15.181, 14.887, 14.642 (av.=14.903)	15.508, 14.417, 14.008 (av.=14.644)

^aFrom reference 22c of the text.

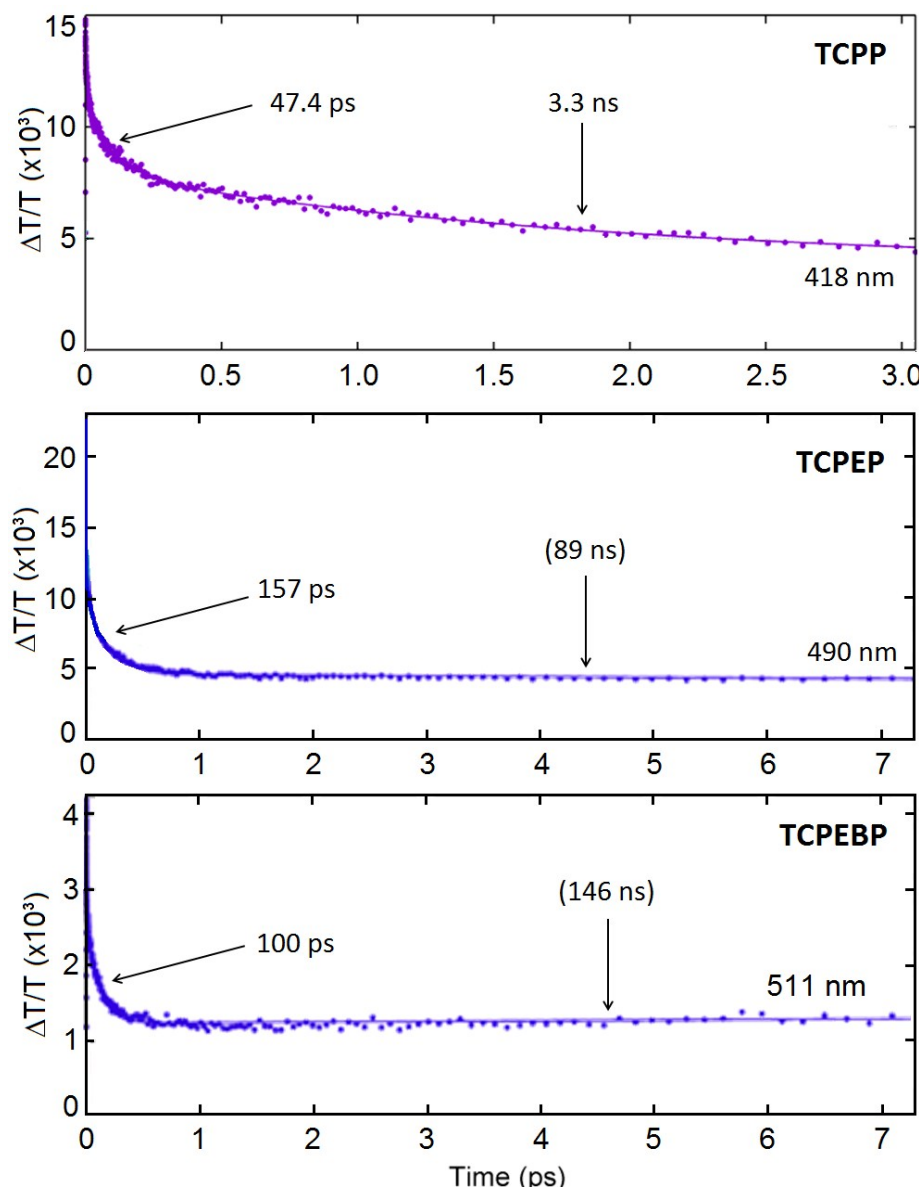


Figure S17. Monitoring of the transient signals of **TCPP**, **TCPEP** and **TCPEBP** in 2MeTHF in the presence of 2 equiv. of [Pd₃²⁺] at 298 K. The monitoring wavelengths are indicated on the graphs. The ps and ns time constants are associated with the charge separation and charge recombination, respectively.